Scit&ncePG
Science Publishing Group

Plant-Based Silver Nanoparticles for the Detection of Lead (II) Ions

Aliyu Muhammad[1, *], Abubakar Umar Birnin-Yauri[1], Hannatu Abubakar Sani[1], Yusuf Haruna[1], Sayudi Yahaya Haruna[1], Abdulmalik Aminu[2]

[1]Department of Pure and Applied Chemistry, Faculty of Physical Sciences, Kebbi State University of Science and Technology, Aliero, Nigeria

[2]Department of Pure and Industrial Chemistry, Faculty of Science, Federal University, Birnin Kebbi, Nigeria

Email address:

amnakowa@yahoo.com (Aliyu Muhammad)

[*]Corresponding author

To cite this article:

Aliyu Muhammad, Abubakar Umar Birnin-Yauri, Hannatu Abubakar Sani, Yusuf Haruna, Sayudi Yahaya Haruna, Abdulmalik Aminu. Plant-Based Silver Nanoparticles for the Detection of Lead (II) Ions. *American Journal of Applied Chemistry*. Vol. 11, No. 3, 2023, pp. 75-80. doi: 10.11648/j.ajac.20231103.11

Abstract: Here in, silver nanoparticles (AgNPs) is synthesized using orange (*Citrus sinensis*) peel as reducing agent and applied in the detection of lead (II) ions in water. A simple technique was used in the synthesis of the said nanoparticles Different analytical techniques such as; UV-Visible Spectroscopy (UV-Vis), Scanning Electron Microscopy (SEM), Fourier Transform Infrared Spectroscopy (FTIR), and X-ray Diffraction (XRD) were used to characterize the as-synthesized AgNPs. FTIR results revealed the fingerprint of the active antioxidants involved in the reduction of silver nitrate to AgNPs. The XRD results shows that silver nanoparticles possess crystalline face centered cubic (FCC) lattice structures. Variable experimental parameters such as; silver ion concentration, pH, incubation time, plant extract volume, and temperature were investigated. The results shows that 1:8 ratio of plant extract volume to silver salt precursor the nanoparticles have yellowish brown and golden brown colors and a surface plasmon peak around 420 nm, SEM images displayed an array of polydispersed spherical AgNPs having an average size of 55 nm. The XRD pattern revealed peaks that are similar to that of silver while FTIR results revealed the functional groups associated with reducing silver ions and stabilizing silver nanoparticles. Colorimetric studies showed that the AgNPs lose their characteristic color when they interact with lead ions, and with the color gone, the surface plasmon resonance (SPR) absorption peak also disappears. A high selectivity and sensitivity were recorded towards Pb (II) ions.

Keywords: AgNPs, Orange Peels, Surface Plasmon Resonance, Lead (II) Ions, Detection, Green Synthesis

1. Introduction

Silver nanoparticles are metal nanomaterials that dominated certain research areas due largely to their promising properties and vast number of applications. These particles possess the ability to strongly absorb electromagnetic waves in the visible region, thus, showing good optical and electrochemical properties coupled with good biological compatibility and high extinction co-efficient [1-3]. The advent of nanomaterials incorporation into sensing systems leads to increase in stability, enhanced sensitivity, and also reduced cost [4].

The persistence nature of lead is of concern largely to human being especially when it comes into contact with soil or water. Contamination of leads comes in different ways some of which include; volcanic eruptions or from human activities that utilizes or produces lead compounds.

Once it enters the environment, lead tends to bio-accumulate and bio-magnify along the food chain with humans being as the major victims. The most common ways through which humans are exposed to lead include; consumption of contaminated fishes, vegetables, inhalation of elemental lead (Pb) and consumption of lead contaminated water. Long time exposure to any form of lead is known to disrupt human nervous system particularly in young children and babies. Potential adverse effects of Pb include learning disabilities, insomnia, and kidney damage, loss of memory, impaired

coordination and negative effects on immune, cardiovascular, and reproductive systems. [5-6]. Different analytical techniques are used in the determination of lead some of which include cold vapor atomic absorption spectroscopy (CVAAS) [7], flame photometry (FP) [8], inductively coupled plasma mass spectrometry (ICP-MS) [9], and high performance liquid chromatography (HPLC) [10]. Even though these techniques appeared to be good they suffered some limitations which include; time consumption, being expensive, and they involved high sample preparation processes. Thus, a simple, fast, and less expensive technique is needed.

Silver nanoparticles have been at the center of interest in colorimetric studies due to the relationship between their characteristic colors and the surface plasmon resonance (SPR) peak [11]. The idea of lead's optical detection by AgNPs involve the reaction of silver with lead to form zero valent lead which leads to decolorization of AgNPs and the loss of SPR peak (Figure 1). The reaction is aided by the unique properties possessed by silver at the nanoscale which favors the formation of silver-lead amalgam [12-13], demonstrated the ability of basil plant extract to reduce silver ions into silver nanoparticles which were applied as nanosensors under biogenic conditions. The synthesized nanoparticles displayed high selectivity in detecting lead ions in the presence of other cations.

2. Materials and Methods

2.1. Chemicals and Solutions

Silver Nitrate (99.8%) was obtained from Sigma Aldrich (USA), Potassium Hydroxide (KOH) and Sulfuric Acid (H_2SO_4) were obtained from Loba Chemicals (India), while Potassium Bromide (KBr) was obtained from Merck (Germany). The metal salts used (NaCl, $CaCl_2$, $MgCl_2.6H_2O$, $AlCl_3.6H_2O$, $Cd(NO_3)_2.4H_2O$, $NiCl_2.6H_2O$, and $Pb(NO_3)$. H_2O were obtained from Sigma Aldrich (USA) corporations. The chemicals were used as received without further purification. All glassware used were washed with distilled water followed by rinsing in dilute nitric acid water prior to experiments.

2.2. Samples Collection

The water sample was collected from Garin Auwal, Fakai Local Government, Kebbi State, Nigeria, while Fresh orange was purchased in Aliero market, Kebbi State, Nigeria.

2.3. Preparation of Orange Peel Extract

The orange was peeled with a clean knife and the peel were cut into smaller pieces and washed with deionized water. 10 g of the peel was boiled in 100 mL of water for 5 minutes followed by filtration to obtain the extract which was used in the synthesis of silver nanoparticles.

2.4. Preparation of AgNPs from Orange Peel

For the biosynthesis of silver nanoparticles, 40 mL of 0.01 M $AgNO_3$ was measured and placed on a magnetic stirrer. 5 mL of orange peel extract was added to the silver salt solution at 50°C and subjected to stirring. The reaction processes were evaluated by color changes of the solution from colorless to yellow to brown and a UV-Vis analysis was used to confirm the formation of AgNPs.

2.5. Study of Variable Experimental Conditions

Here, AgNPs were synthesized using 0.01, 0.02 and 0.03 M $AgNO_3$ at different temperature (25°C, 50°C, and 75°C) and at acidic and alkaline medium of (3, 4, 5) and (10, 11, 12) respectively. Different volumes of plant extracts (3 mL, 5 mL, 7 mL, and 10) were used, reaction time of 2, 5, 10, 20 minutes were also put into evaluation.

2.6. Instrumentation

In this study, UV-Vis analyses were conducted with Thermo Scientific Genesys 10S UV-Visible Spectrophotometer running on VISION Lite software, The X-ray diffraction was done using Rigaku Ultima IV X-ray Diffractometer, Field emission scanning electron microscopy was examined with Quattro S SEM device while FTIR analysis was conducted with Thermo Electron Nicolet 6700 FTIR Spectrophotometer.

2.7. Colorimetric Studies

In the detection of Pb (II) using the as synthesized AgNPs, an aliquot (1 mL) of AgNPs was taken and recorded as blank. To this, 4mL of 1 mM Pb^{2+} was added so as to establish the sensing ability of the silver nanoparticles. This was followed by the addition of 4 mL of solutions containing different Pb^{2+} ions concentrations, so as, to determine the efficiency of the proposed method. Selectivity of AgNPs towards detection of Pb (II) ions was evaluated by addition of cations of representative metals groups; alkali (Na^+), alkali earth (Ca^{2+}, Mg^{2+}, Al^{3+}), and transition (Ni^{2+}, Cd^{2+}) of the same concentration (1 mM) under same experimental conditions. The changes in color were visually observed and the corresponding absorbance changes were confirmed with a UV-Vis spectrophotometer.

3. Results and Discussion

3.1. Synthesis of Silver Nanoparticles

When the plant extracts was added to the solution silver nitrate, a dramitical color change was observed from colorless to light yellow and finally to golden brown. The synthesis reaction was monitored by both color change and UV-Vis spectroscopy. The UV-Vis spectra of silver nanoparticles indicated a broad absorption around 420 nm. This peak corresponds to SPR excitation of AgNPs in aqueous medium, and it is well documented in various literatures with sizes ranging from 2 to 100 nm [14].

3.2. Effects of Physicochemical Parameters

3.2.1. Effect of Silver Ion Concentration

Effect of silver ions concentration on the synthesis AgNPs

as shown in Figure 2, it revealed that as the concentration of silver ions increases, the intensity of the absorption of AgNPs also increases. The AgNPs colloid solution prepared with 0.01 M silver nitrate shows an SPR peak at 438 nm and the intensity of the peaks increases as the concentration increased from 0.01 M to 0.03 M indicating the formation of more AgNPs with increasing concentration of silver salt [15]. This is in agreement with Beer Lambert's Law (A∝C), as the concentration of silver ions increases, the absorbance also increases showing a higher concentration of AgNPs in solution. A similar increase in SPR peak intensity with increasing silver ion concentration has been reported [16].
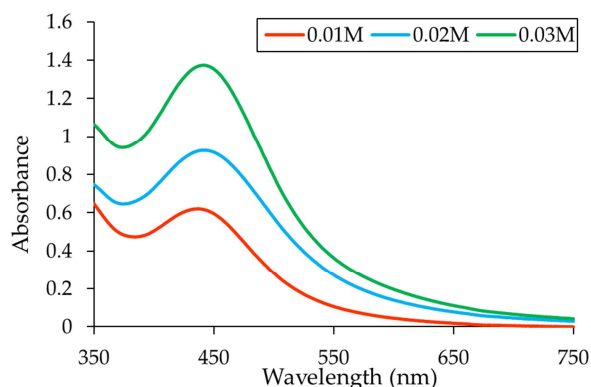

Figure 1. Effect of silver nitrate concentration on Silver Nanoparticles synthesis.

3.2.2. Effect of pH

The next factor evaluated is pH as shown in Figures 3 and 4. In pH studies, the pH conditions of the orange peel extract were varied with dilute sulfuric acid and potassium hydroxide in two different experimental conditions, one in acidic range (pH 3, 4 and 5) and the other in alkaline range (pH 10, 11 and 12). During the synthesis, it was observed that the formation of AgNPs proceeded faster as the pH value becomes more alkaline, hence the reactions conducted in alkaline pH took an average of 3 minutes while the ones conducted under acidic conditions took 15 minutes to complete. At pH 3, a weak peak and light yellow coloration was observed. The observed peaks becomes more intense and the colors changes golden brown as the pH increased to 4 and 5 (Figure 3). The variation in colors can be ascribed to the variations in the pKa values of functional groups of the natural antioxidants present in the Orange peel [17].
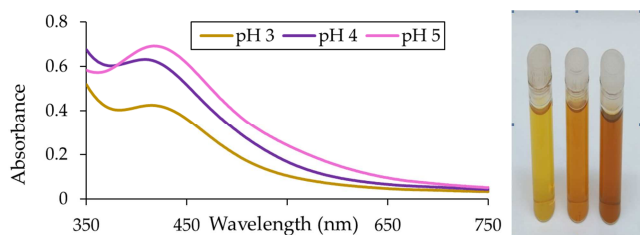

Figure 2. Effect of acidic pH on Silver Nanoparticles (inset shows variations in colors with increase in pH).

Literature shows that, bio-reduction of silver and the subsequent formation of AgNPs in aqueous medium is supported by alkalinity, thus, this can be the basis of the increase in speed of the reaction and the intensity of the peak height under alkaline conditions and the reduction of the speed of reaction and intensity of the peak height in acidic medium. [18]. Alkalinity is known to interfere with the electrostatic repulsion between nanoparticles, there by preventing them from agglomerating [19]. Alkaline medium is said to favored the occurrence of surface plasmon resonance [20]. Particle size is said to be bigger in acidic medium than in basic medium [21]. This suggest why SPR peaks of acidic medium are broad and those of alkaline medium are narrow.
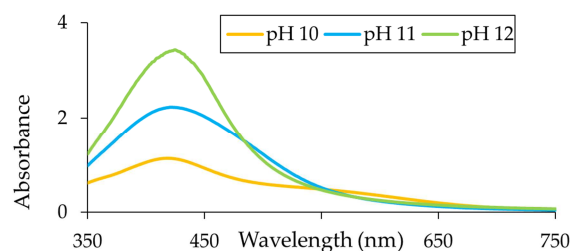

Figure 3. Effect of alkaline pH on Silver Nanoparticles.

3.2.3. Effect of Plant Extract Volume

Figure 4 shows the effect of plant extract volume on silver nanoparticles concentration. It was observed that as the volume of the plant extract increases the absorption peak also increases. When small amount of the plant extract was used, a flat absorption peak was observed suggesting that the amount of the antioxidants present is not sufficient to reduce the silver ions present in the specified volume of silver salt. As the amount the plant extract increases (5 mL) an increase peak height was observed suggesting that higher amounts of the antioxidants responsible for the reducing of the metal ions are present, leading to the formation of AgNPs. Such increase in absorption intensity has been previously reported [21, 19]. This demonstrates that an extract volume of 5 mL is sufficient to reduce 40 mL of silver (II) ion solution, a ratio of 1:8. A decrease in intensity of SPR peaks was observed as the amount of the plant extract was increased to 7 mL and 10 m. This decrease in peak height can be ascribed to the fact that there is dilution of the solution by the quantity of the plant extract added [22].
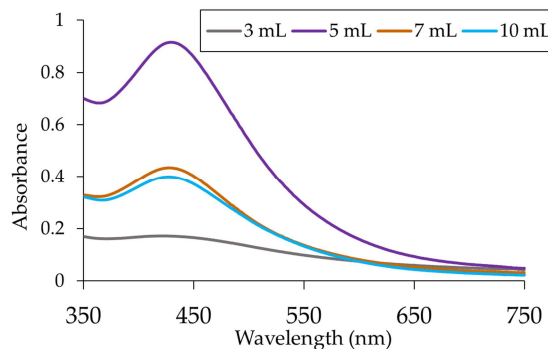

Figure 4. Effect of plant extract volume on Silver Nanoparticles concentration.

3.2.4. Effect of Temperature

The working temperature under which the synthesis of AgNPs was conducted also affected the formation of silver nanoparticles. The observed SPR peaks for the analysis carried out at different temperatures, shows an increase in absorption intensity as temperature increases. At room temperature (25°C), the reaction took 7 minutes to produce a color change and the absorption peak was less pronounced. However, as the temperature reached 80°C, the reduction process went faster; a change in color was noticed within 2 minutes and the peaks became more pronounced. Temperature is an important factor in the synthesis of AgNPs and it favored the rate of the synthesis reaction by inducing rapid reduction of Ag^+ ions into AgNPs. Reports have shown that an increase in temperature leads to a decrease in the size of silver nanoparticles [23]. This is due to the fact that as the temperature increases, the reaction proceeds more rapidly which leads to the homogenous nucleation of silver nuclei thereby leading to the formation of small-sized silver nanoparticles [24].

3.2.5. Effect of Reaction Time

Influence of reaction time on the synthesis of AgNPs was evaluated at intervals of 2, 5, 10, 20, 40, and 80 minutes. The result showed a systematic increase in color intensity as the incubation time increases. The bands formed at 2, 5, 10, and 20 minutes incubation time are within the range of 430 – 440 nm while those taken at 40 and 80 minutes showed a gradual shift below 430 nm. This decrease in AgNPs size over time and similar trend has been reported [21]. The increase in absorbance could be attributed to an increase in the quantity of silver nanoparticles as the reaction progresses. There were concerns that as the incubation time increases, there is a big tendency for agglomeration of AgNPs thereby leading to the formation of bigger sized particles.

3.3. Silver Nanoparticles Characterization

The optimized experimental conditions were used for synthesis of AgNPs used for characterization and colorimetric studies. The optimized conditions are; 0.01 M concentration $AgNO_3$, 1:8 volumetric ratio of orange peel extract to silver salt, a temperature of 50°C, a pH of 10 and a reaction time of 4 minutes.

3.3.1. Fourier Transform Infrared Spectroscopy (FTIR)

The spectra obtained from FTIR analysis shows a broad peak arising at 3433 cm^{-1} which can be ascribed to the presence of hydroxyl (OH) groups attached to the phenols present in the extract. Within the same range, symmetric and asymmetric vibration modes of aliphatic C-H groups were observed at frequencies of 2923 cm^{-1} and 2855 cm^{-1} [25]. The peak occurring at 1629 cm^{-1} can be assigned to the amide I band which correspond to the C=O stretching associated with proteins, it may also be due to the aromatic C-C bending of flavonoids which are one of the major constituents of orange peels. The peak at 1380 cm^{-1} is related to the amide III band (1400 – 1200 cm^{-1}) which consist of the in-phase coupling of

N–H bending and C–N stretching. The findings gave an insight into the functional groups that per take in the synthesis reaction and they specifically highlight the involvement of protein molecules in the stabilization of AgNPs through amide bonds. Orange peels are mainly composed of flavonoids, monoterpenes, alkaloids, hesperidin, phenols, and these biomolecules are known to interact with metal salts to yield silver nanoparticles as documented in previous studies [21].

3.3.2. X-ray Diffraction (XRD)

The XRD pattern obtained from X-ray diffraction analysis displayed three intense and sharp peaks and one less defined peak. The diffraction peaks obtained at 2θ angles of 37.11^0, 40.86^0, 67.05^0, and 79.17^0 corresponded to the 111, 200, 220, and 311 miller indices. The observed peaks point to the high crystallinity of the silver nanoparticles and peaks arising from impurities were not detected. The narrowness of the peaks indicates a smaller sized silver nanocrystals. This is based on Scherrer's equation which asserts that the peak width is a major determinant that reveals the size of nanoparticles crystallites. The patterns reveal good similarity with two different International Center for Diffraction Data (ICDD) files; 87-0717 and 87-0718 [26, 25]. According to the ICDD references, the analyzed silver nanoparticles exhibits a face-centered cubic lattice structure.
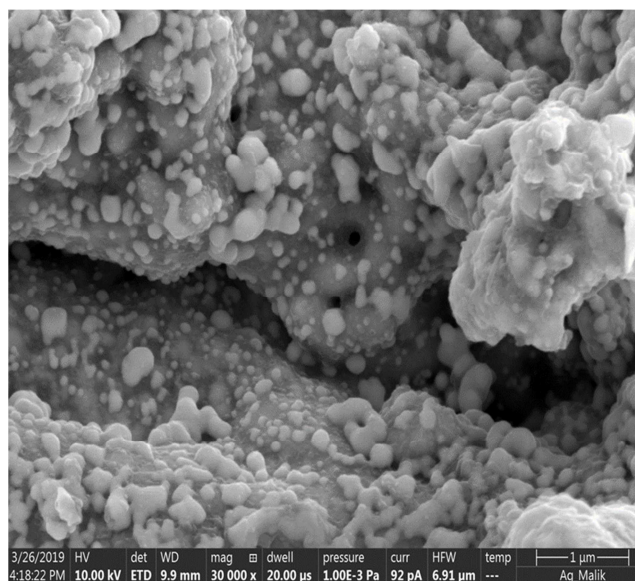
3.3.3. Scanning Electron Microscopy (SEM)

Figure 5. SEM image of the synthesized Silver Nanoparticles.

Scanning electron microscope was used to analyzed the surface morphology and distributions of the synthesized silver nanoparticles. SEM image obtained at 30000 magnification revealed an array of polydisperse AgNPs (Figure 5). From the images it is observed that some of the nanoparticles agglomerated into nanoclusters, which can be attributed to the longer incubation time which the nanoparticles were subjected to. It might also have arisen from the sample preparation method used for the SEM

analysis. Majority of the nanoparticles are spherical in shape but some were found to possess irregular shapes, and their average size were estimated to be 55 nm. The morphology of the AgNPs was found to be poorly defined and irregular. [21] also reported a similar occurrence in biosynthesized silver nanoparticles and ascribed it to the numerous reduction routes that silver ions may follow in a complex solution that contains multiple reducing agents like citric acid, flavonoids, and hesperidin.

3.4. Colorimetric Detection of Lead (II) Ions by AgNPs

The colorimetric analysis conducted using asynthesized silver nanoparticles showed a remarked variation in UV-Vis response and color of the solution after the addition of Pb (II) ions. As can be observed from Figure 7, lead ions caused a sudden change in color from golden brown to light brown and finally to colorless within 2 minutes and the SPR peak also disappeared in the absorbance spectrum. This suggests that the AgNPs can be used for the detection of Pb (II) ions. However, other cations (Na^{2+}, Ca^{2+}, Mg^{2+}, Al^{3+}, Cd^{2+}, Ni^{2+}) showed no such effect on neither the color nor the absorbance peaks of silver nanoparticles, signaling that the observed changes are peculiar to a specific interaction between lead and nanoscale silver. It may be inferred that the selectivity of AgNPs towards lead (II) ions is basically built due largely to its ability to form the silver-lead amalgam [27], because other metallic cations lack the capacity to form amalgams with silver, thus, do not cause a significant change in color or loss of SPR peaks as they interact with silver nanoparticles [28].
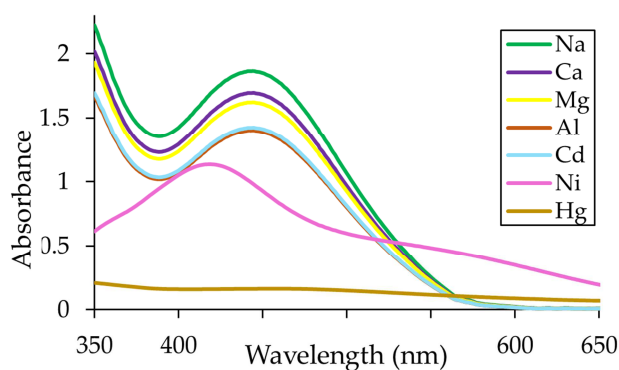

Figure 6. SPR spectra of silver nanoparticles with various metal cations.

The change in absorbance plotted for every metal cation showed that the largest difference was observed in lead due to the complete loss of SPR peak which led to a flat absorbance response (Figure 6).

For the determination of the sensitivity of synthesized AgNPs towards Pb (II), the concentration of lead (II) ion was varied from 1 μM to 100 μM. It was found that with every increase in the concentration of Pb^{2+}, there is a drop in absorbance intensity and the color of the solution changes dramatically. The variation in concentration was found to produce a linear response within the range of 1 μM to 100 μM ($R^2 = 0.9818$) (Figure 7).

4. Applicability Test

Effectiveness of the proposed method was evaluated by detection of Pb (II) ions in spiked water samples. Here, a complex matrix of different metals was formed to test the possibility of interference from other metal ions. Equal volumes each of 1 mM solutions of Na^{2+}, Ca^{2+}, Mg^{2+}, Al^{3+}, Cd^{2+}, Ni^{2+} and Pb^{2+} were mixed together and added to 1 ml of AgNPs. Another solution was made in which all the above mentioned metal ions with the exception of lead were mixed and added to silver nanoparticles, and a third solution was made which contained AgNPs and Pb only. Figure 7 displays the corresponding UV-Vis spectra for all the three solutions. Presence of interfering species cannotreduce the capability of the proposed sensor towards detection of Pb (II) ions.
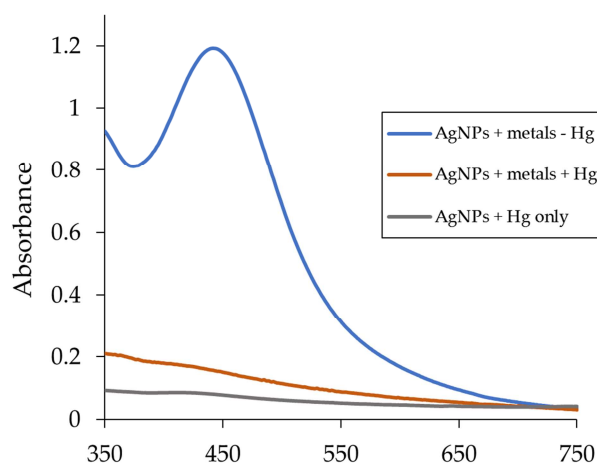

Figure 7. SPR spectra of interference test.

5. Conclusion

An optical sensor with the ability to detect Lead (II) ions in water is developed using plant based AgNPs. The developed sensor exhibits high selectivity and sensitivity in detection of Pb (II) ions in water, the sensor is also found to be economical with short response time. The result obtained in the analysis of Lead (II) ions in water shows the reliability of this sensor in the detection of lead (II) ions in water. Thus, the sensor can be applied for environmental monitoring and quality control.

Acknowledgements

References

[1] Annadhasan M., T. Muthukumarasamyvel, V. R. Sankar Babu and N. Rajendiran, (2014). *ACS Sustain. Chem. Eng. 2*, 887. doi: 10.1021/sc400500z.

[2]   Mohammed MB, Volkov V, Link S, Sayed MAE. (2000). The 'lightning' gold nanorods: fluorescence enhancement of over a million compared to the gold metal. *Chem. Phy. Lett. 317*: 517-523.

[3]   Rai M, Gade A, Yadav A. (2011). Biogenic nanoparticles: an introduction to what they are, how they are synthesized and their applications in microbiology. *Springer, Berlin*, pp. 1-16.

[4]   Yunus, I. S, A. Kurniawan Harwin, D. Adityawarman, A. Indarto. (2012). Nanotechnologies in water and air pollution treatment. *Environ. Tech. Rev. 1*. 136-148.

[5]   Kendall M, and Holgate S. (2012). Health impact and toxicological effects of nanomaterials in the lung. *Respirology. 17*: 743-758.

[6]   Zahir F., Rizwi, S. J., Haq, S. K., and Khan, R. H. (2005). Low dose lead toxicity and human health. *Environmental Toxicology and Pharmacology*, *20* (2), 351-60.

[7]   Yamini, Y, N. Alizadeh, M. Shamsipur. (1997). Solid phase extraction and determination of ultra-trace amounts of lead (II) using octadecyl silica membrane disks modified by hexathia-18-crown-6-tetraone and cold vapor atomic absorption spectrometry. *Anal. Chim. Acta 355*, 69-74.

[8]   Kuswandi, K., A. Nuriman, H. H. Dam, D. N. Reinhoudt, W. Verboom. (2007). Development of a disposable lead ion-selective optode based on trityl-picolamide as ionophore. *Anal. Chim. Acta, 591*, 208–213.

[9]   Fong, B., W. Mei, T. S. Siu, J. Lee, K. Sai, S. Tam. (2007). Determination of lead in whole blood and urine by inductively coupled plasma mass spectrometry. *J. Anal. Toxicol. 31*, 281–287.

[10] Ichinoki, S., N. Kitahata, Y. Fujii. (2004). Selective determination of lead (II) ion in water by solvent extraction followed by reversed-phase HPLC. *J. Liq. Chromatogr. Rel. Technol. 27*, 1785-1798.

[11] Aslan, K., J. R. Lakowicz, C. D. Geddes. (2004). Nanogold–plasmon-resonance-based glucose sensing. *Anal. Biochem. 330*, 145-155.

[12] Park Y. (2014). New paradigm shift for the green synthesis of antibacterial silver nanoparticles utilizing plant extracts. *Toxicol. Res., 30*: 169-178.

[13] Omobayo S. A., Chanbasha B., Khan Z., Abdulnaser A., Zia S. (2016). Biogenic synthesis of silver nanoparticles; study of the effect of physicochemical parameters and application as nanosensor in the colorimetric detection of Pb^{2+} in water. *International Journal of Environmental Analytical Chemistry, 96*: 8, 776-788.

[14] Park, Y.; Hing, Y. N.; Weyers, A.; Kim, Y. S.; Linhardt, R. J. (2011). Polysaccharide and phytochemicals: A natural reservoir for the green synthesis of gold and silver nanoparticles. *IET Nanobiotechnol. 5* (3), 69-78.

[15] Zaki S, El-Kady MF, Abd-El-Haleem D. (2011). Determination of the effective origin source for nanosilver particles produced by Escherichia coli strain S78 and its application as antimicrobial agent. *Mater. Res Bull., 46*: 1571-1576.

[16] Dubey, M.; Bhadauria, S.; Kushwah, B. S. (2009). Green synthesis of nanosilver particles from extract of Eucalyptus hybrida (Safeda) leaf. *Dig. J. Nanomater. Biostruct. 4 (3),* 537-543.

[17] Pimprikar, P. S., Joshi, S. S., Kumar, A. R., Zinjarde, S. S., and Kulkarni, S. K. (2009). Influence of biomass and gold salt concentration on nanoparticle synthesis by the tropical marine yeast Yarrowia lipolytica NCIM 3589. *Colloids and Surfaces, B: Biointerfaces, 74*, 309e316.

[18] Huang JL, Li QB, Sun DH, Lu YH, Su YB, Yang X. (2007). Biosynthesis of silver and gold nanoparticles by novel sundried Cinnamomum camphora leaf. *Nanotechnology 18* (10), 105-106. http://dx.doi.org/10.1088/0957-4484/18/10/105104

[19] Sathishkumar, M.; Sneha, K.; Yun, Y. S. (2009). Palladium nanocrystals synthesis using Curcuma longa tuber extract. *Int. J. Mater. Sci., 4* (1), 11-17.

[20] Vanaja, M.; Annadurai, G. (2012). Coleus aromaticus leaf extract mediated synthesis of silver nanoparticles and its bactericidal activity. *Appl. Nanosci.*, DOI: 10.1007/s13204-012-0121-9.

[21] Abdulmalik A. Sulayman A. O. (2020). Fast Orange Peel-Mediated Synthesis of Silver Nanoparticles and Use as Visual Colorimetric Sensor in the Selective Detection of Mercury (II) Ions", *Arabian Journal for Science and Engineering*, 46, 5477-5487.

[22] Noruzi, M., Davood Z, Kamyar K, Daryoush D. (2011). Rapid green synthesis of gold nanoparticles using Rosa hybrida petal extract at room temperature. *Spectrochimica Acta Part A, 79*, 1461-1465.

[23] Fayaz AM, Balaji K, Kalaichelvan PT, Venkatesan R. (2009). Fungal based synthesis of silver nanoparticles — an effect of temperature on the size of particles. *Colloids Surf B; 74:* 123-6.

[24] Jiang H, Manolache S, Lee Wong AC, Denes FS. (2004). Plasma enhanced deposition of silver nanoparticles onto polymer and metal surfaces for the generation of antimicrobial characteristics. *J. Appl. Polym. Sci., 93*: 1411-1422.

[25] Dhand V, Soumya L, Bharadwaj S. (2016). Green synthesis of silver nanoparticles using coffee arabica seed extract and its antibacterial activity. *Mater. Sci. Eng, C., 58*: 36-43.

[26] Gopinatha V, Ali MD, Priyadarshini S, Meera Priyadharsshini N, Thajuddinb N, Velusamy P. (2012). Biosynthesis of silver nanoparticles from Tribulus terrestris and its antimicrobial activity: a novel biological approach. *Colloid Surf B: Biointerface, 96* (69-74).

[27] Rastogi R. B. L., Sashidhar, D., Karunasagar and J. Arunachalam, (2014). Gum kondagogu reduced/stabilized silver nanoparticles as direct colorimetric sensor for the sensitive detection of Pb^{2+} in aqueous system. *Talanta, 118*, 111-117. doi: 10.1016/j.talanta.2013.10.012.

[28] Farhadi K., M. Forough, R. Molaei, S. Hajizadeh, A. Rafipour. (2012). *Sens. Actuators B., 161*; 880-885.